https://doi.org/10.20965/jrm.2015.p0259

Paper:

Impact Piezo-Driven Micro Dispenser and Precise Miniature *XY* Stage

Yuuka Irie*, Shinnosuke Hirata, Chisato Kanamori*, and Hisayuki Aoyama***

*Department of Mechanical Engineering and Intelligent Systems, The University of Electro-Communications
1-5-1 Chofugaoka, Chofu, Tokyo 182-8585, Japan
E-mail: {irie@sys., kanamori@, aoyama@}mce.uec.ac.jp
**Department of Mechanical and Control Engineering, Tokyo Institute of Technology
S5-17, 2-12-1 Ookayama, Meguro-ku, Tokyo 152-8552, Japan
E-mail: shin@ctrl.titech.ac.jp
[Received December 2, 2014; accepted March 19, 2015]

Recently, micro-droplet dispensation has been required in printed-electronics (PE) technology. Devices with micro dispensing mechanism are of key importance in achieving a higher performance with these products. In fact, it is very difficult for the conventional dispenser to squeeze highly viscous liquid with picoliter resolution. This paper describes the development of a dispensing mechanism comprising a dispensing device and *XY* stage, both driven by the piezo impulsive force. The dispensing device is mainly composed of a pipette and a taper needle that is driven by a piezoelectric element. When the needle passes through the pipette, a droplet of the liquid adheres to the needle-tip end. A micro droplet can be transcribed to a target surface by bringing the droplet at the needle-tip end in contact with the target surface. On the contrary, in the *XY* stage, the small tables on the V-shaped grooves can be driven by the impulsive force generated by the mass connected to the piezoelectric element. The *X* stage is stacked on the *Y* stage, which allows fine positioning in the plane. In the experiment, an array of a small amount of 0.2-picoliter droplets was successfully developed on the glass plate.

Keywords: micro dispenser, printed-electronics technology, piezo-impact drive mechanism, needle, highly viscous liquid

1. Introduction

Printed-electronics (PE) technology is based on techniques similar to conventional printing machines. PE technology has the potential for low energy consumption, substantial resource saving, and low environmental impact. Various electronic devices, including thin-film transistors (TFT), printed circuits, displays, optical nanofibers, and sensors, have been fabricated using printing methods such as ink-jet printing, screen printing, and offset printing [1, 2]. For electronic devices, a micro-dispenser mechanism is required for applying liquids with high viscosity, such as glue and metal paste [3]. However, it is very difficult for conventional dispensers such as ink-jet and syringe dispensers to apply highly viscous liquids with picoliter resolution. In these dispensers, there is a trade-off between the liquid viscosity and droplet volume [4]. Ink-jet dispensers can generate small droplets with only low-viscosity inks. Low-viscosity liquids of electrically-conductive material spread easily and become thin, increasing the resistance of the metal wiring pattern. Thus, a small amount of highly viscous liquid should be dispensed on the micro circuit to lower the electrical resistance. Accordingly, a new dispenser mechanism for high-viscosity liquid is required for such micro products in printed electronics.

A micro pump that was inertially driven by piezoelectric elements was developed [5]. However the pump can not push out a small amount of liquid.

We developed a micro-dispenser mechanism, comprising a pipette and needle that is inertially driven by piezoelectric elements so that it can push out a very small amount of highly viscous liquids. A small amount of liquid can be transcribed to a target surface by bringing the needle-tip droplet into contact with the target surface.

In this paper, we describe a micro-dispenser mechanism with an inertially driven micro *XY* stage and a micro-dispenser device with a needle and pipette. In our experiment, we used an electrically conductive paste (50,000 mPas) as the high-viscosity liquid. Our goal was to dispense a small amount of liquid using a needle with a tip diameter of 10 μm. The needle was tapered by electrical-chemical etching. The needle had a maximum diameter of 300 μm.

First, the appropriate waveform for controlling the piezoelectric element that can drive the small slider with the needle is discussed. Then, the actual movement of the small slider is examined using the displacement sensor. After combining the slider with the impact-driven *XY* stage, the array of the micro droplet is examined experimentally. In the primary experiment, the small array of the 0.2-picoliter micro droplet is successfully achieved on the glass plate with 50 μm of space.

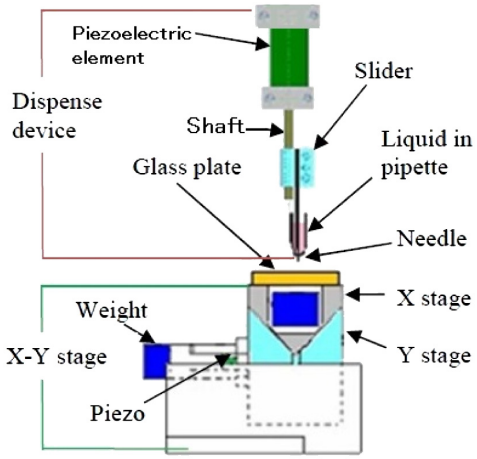

Fig. 1. Micro dispensing mechanism.

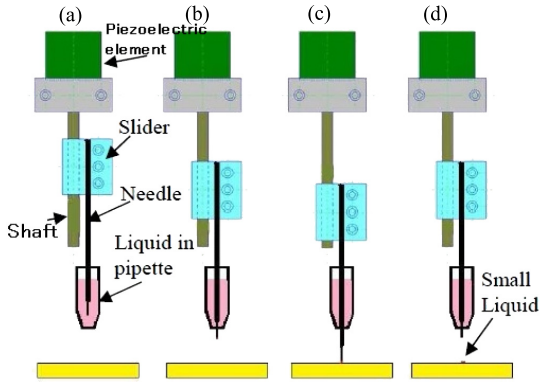

Fig. 2. Principle of dispense device.

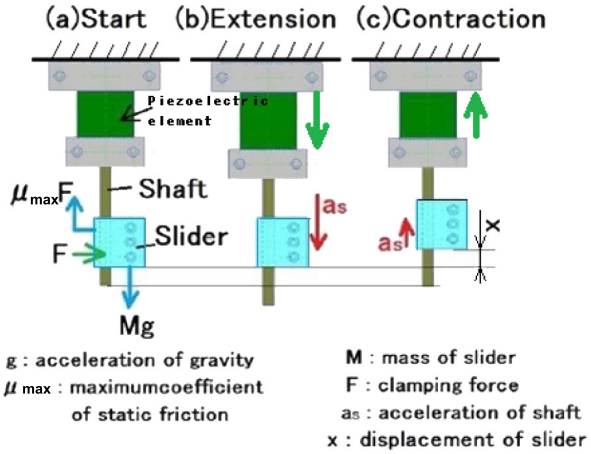

Fig. 3. Principle of dispense device with piezo-impact drive mechanism.

2. Dispense-Device Design

As shown in **Fig. 1**, the micro dispensing mechanism is composed of the dispense device and XY stage, which are both driven by the impulsive force generated by the piezo-impact drive mechanism. This mechanism is well known as the locomotion method for positioning devices. It utilizes the frictional and inertial force caused by the rapid deformations of the piezoelectric element. For example, the mechanism is driven with the force of inertia produced on vibrating a piston of linear type actuator [6]. The mechanism is driven with friction control [7]. This mechanism is not limited to movements in a plane; it is also applicable for the tilting motion for SEM operation [8]. The tilting stage has 0.001° resolution [9]. The standard deviation of angle is 0.729°, and linearity is 0.010 [10]. The arm of micro robot is driven with Impact Drive Mechanism [11]. Konica-Minolta developed a Smooth Impact Drive Mechanism. A lens is attached to this mechanism [12].

The small slider with the needle is clamped with screws onto the shaft connected to the piezoelectric element. The slider can be precisely driven upward and downward by the impulsive force. In the XY stage, the small tables on the V-shaped grooves can be driven by the impulsive force generated by the mass connected to the piezoelectric element. The X stage is stacked on the Y stage, which allows fine positioning in a plane. On the upper stage, the glass plate can be installed. The thin needle passes through the pipette, and then a droplet of the liquid adheres to the needle tip.

Figure 2 illustrates the principle behind dispensing a small amount of the liquid in the pipette. **Fig. 2(a)** shows the initial position. In **Fig. 2(b)**, when the voltage is supplied to the piezoelectric element, the needle can move downward in the pipette. In **Fig. 2(c)**, when the needle passes through the pipette, a droplet of it adheres to the needle tip. When the needle of the dispense device contacts the glass-plate surface, the liquid at the tip of the needle is transferred onto the glass plate. A contact-detection method for the needle-tip droplet and glass-plate surface is implemented using microscopic images. When a needle tip contacts a target surface, the shape of liquid of needle tip is changed. We check the shape of liquid of needle tip using microscopic images.

In **Fig. 2(d)**, the needle can move upward in the pipette.

Figure 3 illustrates the principle of the dispense device with the piezo-impact drive mechanism. The needle is attached to the slider, which can be driven precisely by the impulsive force with the piezoelectric element. The slider is clamped onto the shaft connected to the piezoelectric element. When an input signal such as a saw-tooth waveform is supplied to the piezoelectric element, the slider can move in a stick-and-slip manner.

In **Fig. 3(a)**, at first, the piezoelectric element is fixed with high stiffness to the upper side. The piezoelectric element is not to be elastic deformation and vibration.

The initial clamping force should be such that the slider cannot be pulled down by the gravity force. The clamping force F can be estimated as follows:

$$\mu_{\max} F > Mg \quad \ldots\ldots\ldots\ldots\ldots\ldots \quad (1)$$

M : mass of slider
F : clamping force
g : acceleration of gravity
$\mu_{\max}$: maximum coefficient of static friction

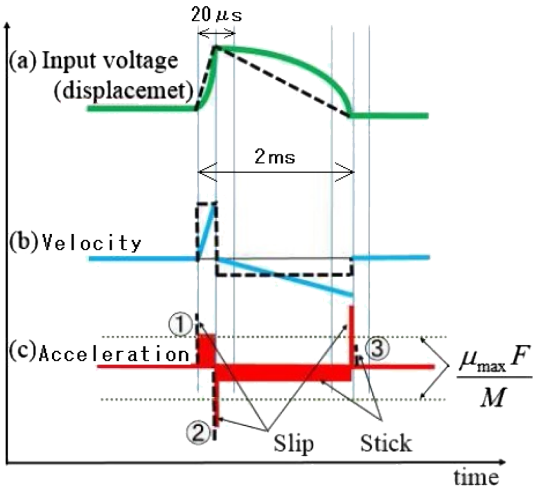

Fig. 4. Saw-tooth waveform for inertia drive.

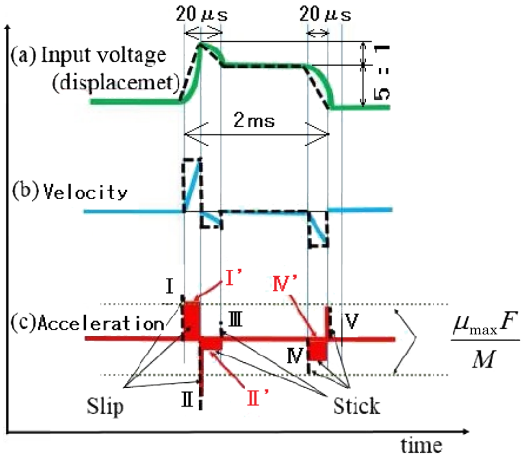

Fig. 5. Square waveform overlaid with impulse input at first point.

When the needle passes through the highly viscous liquid, it experiences viscous resistance. When we use liquid of 50,000 mPas and a needle of $\varphi = 300$ μm, the viscous-resistance force is 1/100 of $\mu_{\max}F$. Thus, the viscous-resistance force is negligible.

In **Fig. 3(b)**, the voltage is applied to the piezoelectric element so that the shaft can be extended with a large acceleration. Then, the slider can generally slip and stay at this position according to the law of inertia. The acceleration of the shaft a_s is estimated as follows:

$$a_s > \frac{\mu_{\max}F}{M}. \quad \ldots\ldots\ldots\ldots\ldots\ldots \quad (2)$$

In **Fig. 3(c)**, the voltage is applied to the piezoelectric element so that the shaft contracts with a small acceleration. The slider can move together with the shaft because of the frictional force. The slider can move the same amount as the displacement of the piezoelectric element.

$$a_s < \frac{\mu_{\max}F}{M} \quad \ldots\ldots\ldots\ldots\ldots\ldots \quad (3)$$

The popular saw-tooth input waveform for the inertially driven method is shown in **Fig. 4(a)** [13]. When the displacement of the piezoelectric element can be ideally given, as for the saw-tooth curve, the velocity and acceleration can be represented by the dashed lines in **Figs. 4(b)** and **(c)**. When the piezoelectric element extends and contracts, large accelerations (①, ②) occur. When this acceleration is bigger than the acceleration at which the slider can be clamped, the slider can generally slip and stay in its position according to the law of inertia. When the piezoelectric element contracts with a constant velocity, the acceleration is not given. When the displacement is zero, the velocity becomes zero, yielding a small acceleration (③). When the piezoelectric element contracts, the slider can be clamped onto shaft and moved. By repeating this operation, precise locomotion movement by a small amount can be performed.

In a real experiment, the electrical circuit for driving the piezoelectric element has a delay time. Moreover, the mechanical dynamics of the mass and the piezoelectric element must be considered. Hence, the real displacement of the piezoelectric element is considered as the solid curve in **Fig. 4(a)**. The time response of the displacement of the piezoelectric element can be represented simply as a quadratic curve [14]. The velocity and acceleration are indicated by the solid lines in **Figs. 4(b)** and **(c)**. When the piezoelectric element extends and contracts and when the displacement returns to zero, large accelerations (② and ③) in opposite directions occur. These large accelerations in opposite directions indicate that the slider is slipping unsteadily. This behaviour has been observed very often in real experiments.

We propose a new waveform, i.e., the square waveform with an impulse signal added on the first point, as shown in **Fig. 5**. The input signal to the circuit can be represented by the dashed lines in **Fig. 5**. The real displacement, velocity, and acceleration that determine the delay time of the voltage circuit and the dynamic mechanical characteristics are indicated by the dashed lines in **Fig. 5**. In the case of this waveform, when the piezoelectric element extends and contracts, a large acceleration (I, I', II) occurs. When this acceleration is larger than the acceleration at which the slider can be clamped, the slider can generally slip and stay in its position according to the law of inertia. The accelerations at II', III, IV, IV', and V are smaller than this large acceleration at I and II. Thus, the slider can be clamped onto the shaft and moved. With this waveform, one step movement of the slider is smaller than the total stroke of the piezoelectric element. We considered in order that it can be moved by the inertial force generated only once per cycle, and stable, and can be moved.

3. Experimental Results

In **Fig. 6**, the slider with a tapered needle driven by the piezoelectric element (AE0505D08F NEC Tokin) is shown. The slider is clamped onto the shaft with screws. It has two adjusting screws and one locking screw. The slider can be moved by the piezo-driven impulsive force.

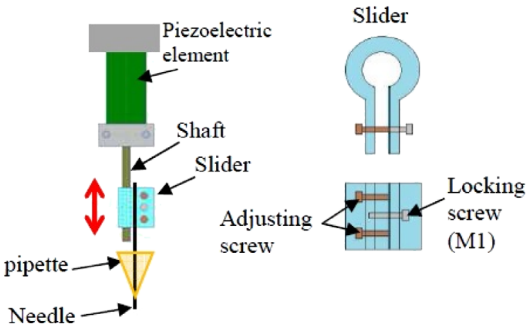

Fig. 6. Layout of dispense device.

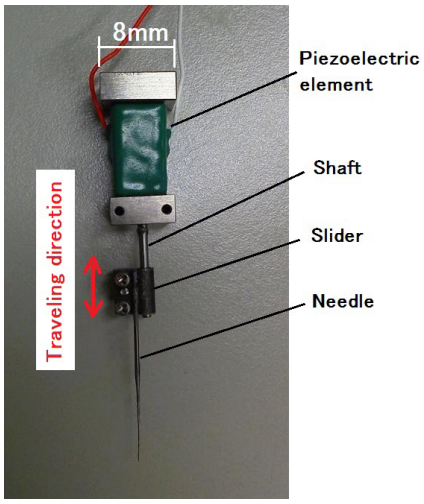

Fig. 7. Slider with taper needle.

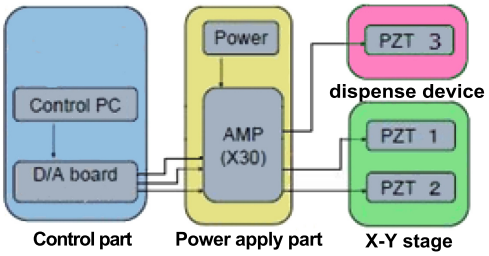

Fig. 8. Control diagram for dispensing mechanism.

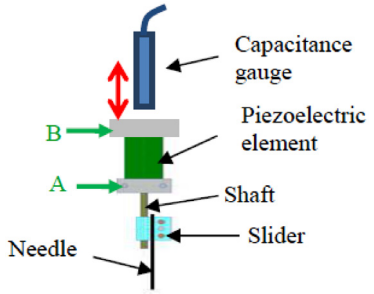

Fig. 9. Layout of measurement.

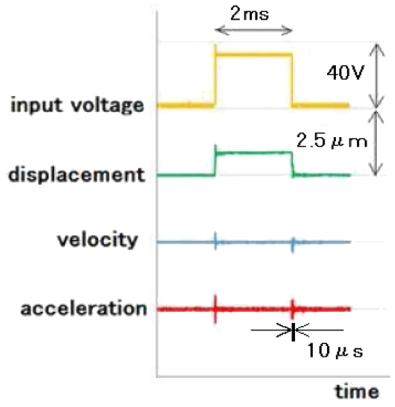

Fig. 10. Relation among input voltage, displacement, velocity, and acceleration.

As shown in **Fig. 7**, the shaft is 1 mm in diameter, 10 mm long, and 0.06 g in weight. The slider is 5 mm in length and height, 1.3 mm in width, and 0.21 g in weight. The shaft and slider are made of SUS303. A sapphire is often used for guide face in industrial application. A sapphire has a performance of less-attrition and less-deterioration. The shaft and the slider made from SUS303 have similar performance and can be machined easily with low cost. The locking screw is an M1 (pitch = 0.25 mm, pitch diameter of thread = 0.838 mm). The needle is 0.3 mm in diameter, 20 mm long, and 0.01 g in weight.

An input waveform was generated by a PC with a D/A board and applied to the piezoelectric elements of the dispensing mechanism, as shown in **Fig. 8**.

The sampling rate of the D/A signal-converter board is 10 μs, and the static-current capacity of the electric amplifier is 0.1 A for each actuator. The slew rate of this electric amplifier under the capacitance load is 4000 V/s. This performance is good enough to drive such a piezoelectric element with mechanical dynamics.

A commercial capacitance gauge (ADE 3046-A02) is employed for measuring the displacement of this piezoelectric element, as shown in **Fig. 9**. Rather than the displacement of the needle, the displacement of the other end of the piezoelectric element is measured by fixing the point A. When the slider can be driven by the impulsive force, the piezoelectric element is fixed at the point B.

In **Fig. 10**, when 40 V is applied, the piezoelectric element can be expanded by approximately 1 μm.

The acceleration time is 10 μs in **Fig. 10**. The maximum coefficient of the static friction was measured from the experiments ($\mu_{\max} = 0.42$). The slider weighs 0.21 g ($M = 0.21$). The clamping force F is adjusted to satisfy Eqs. (2) and (3).

As shown in **Fig. 11**, the laser-displacement sensor (LK-G35 Keyence Inc.) is set up in the traveling direction to check the slider motion. As shown in **Figs. 12(a)** and **(b)**, the displacement of the slider was measured by checking the positions while the slider moved a certain distance along the traveling direction. The time interval of the square waveform and the impulse signal added on

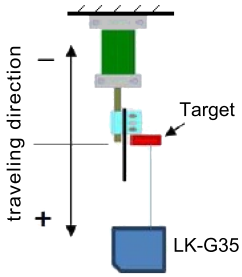

Fig. 11. Measuring method using laser displacement gauge.

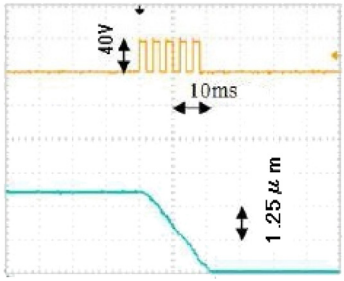

(a) Slider moves upwards

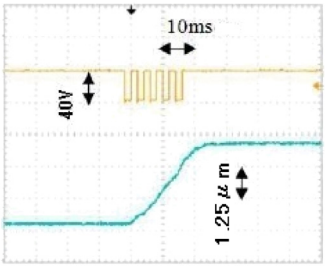

(b) Slider moves downwards

Fig. 12. Displacement of slider.

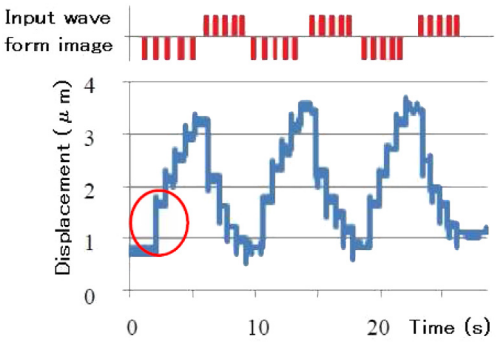

Fig. 13. Close up displacement of the impact driven slider.

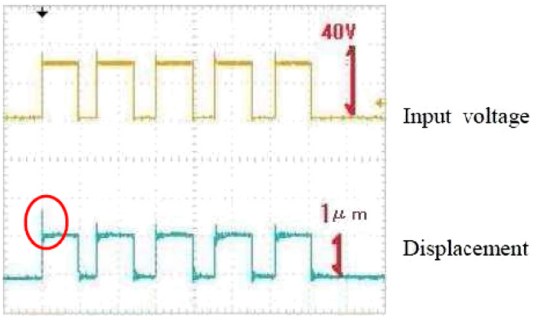

Fig. 14. Response of piezoelectric element to the square waves.

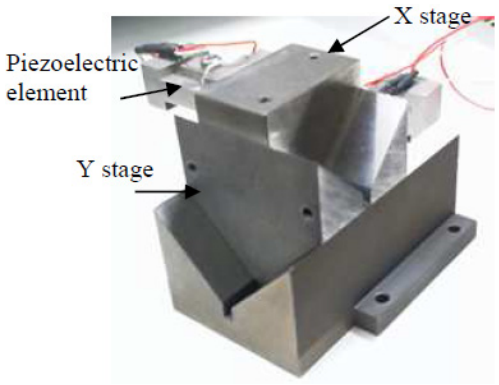

Fig. 15. Inertially driven *X*-*Y* stage.

the first point was 2 ms. The measured response of the moving slider was the slope line due to the delay of the laser-displacement sensor and the mechanical-system response.

The step movement is shown in **Fig. 13**. Here, the slider can move downward and upward in several steps with a time interval of 1 s so that each step can be measured clearly. When the displacement of the slider was observed microscopically, the first steps of the displacement were bigger than the other steps owing to the hysteresis loop of the piezo element.

It was found that the slider has a good repeatability of movement, which means that it has been cramped onto the shaft with no such backlash. As shown in **Fig. 14**, the displacement of the piezoelectric element was measured according to the layout of **Fig. 9**. The input voltage was not changed, but at the first impulse input, the displacement became larger than that at the 2nd and 3rd waveforms. It can be considered that there is a certain hysteresis loop of the piezoelectric elements' characteristics, and thus, the first displacement becomes larger than the others. In **Fig. 9**, the first impulse displacement is depicted as smaller than the real displacement because of the sampling rate of the digital-oscilloscope stage.

4. Inertially Driven *X*-*Y* Stage

The micro dispensing mechanism is composed of the dispense device and the *XY* stage. As shown in **Fig. 15**, the *X*-*Y* stage is mainly composed of the inertial mass driven by the piezoelectric elements. The *X* stage is stacked on the *Y* stage, which allows fine positioning in the plane. On the upper stage, the glass plate can be installed. The performance of this *XY* stage was discussed in our previous works [15]. The typical positioning resolution was 0.1 μm in the *X* and *Y* directions with a working range of 15 to 26 mm.

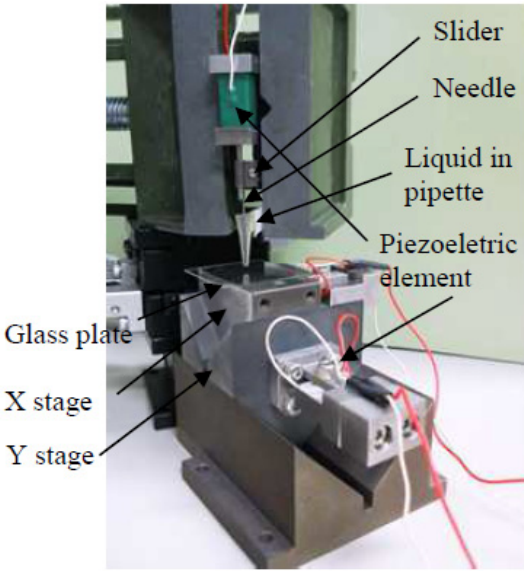

Fig. 16. Micro dispense mechanism.

Fig. 17. Liquid at the tip of a needle is transferred.

5. Micro Dispensing Mechanism and Pattern Making

Figure 16 shows the experimental setup for dispensing the small liquid by the needle. As the primary experiment, the needle was attached to the slider, and the highly viscous liquid (5000 mPas, silicone oil) was transferred onto the glass plate, as shown in **Fig. 17**. There was a small gap between the needle-tip end and glass plate. This dispensing gap is very important and must be controlled precisely for the micro-droplet dispensation. The needle-tip end is monitored by a zooming microscope (VH-Z50R, Keyence Inc.) in order to ensure that the accurate amount of liquid is used for the droplet. The initial gap is determined according to the needle diameter. A small needle diameter requires a narrow initial gap between the needle end and the target surface [16]. As shown in **Fig. 18**, when a needle-tip 300 μm in diameter is implemented, the initial gap is adjusted to $\sim$20 μm. A laser microscope (VK-3510, VK-8550, Keyence Inc.) is employed for measuring the diameter of the needle and the volume of the small liquid. As shown in **Fig. 19**, a micro droplet with a diameter of 350 μm was successfully dispensed on a glass plate with a space of 650 μm under open-loop control. The standard deviation of the mean of the droplet diameter and the position of the droplet were 7 and 1 μm, respectively. The volume of the small liquid was estimated as 960 picoliters, as shown in **Fig. 20**. The thickness of this small liquid was 10 μm.

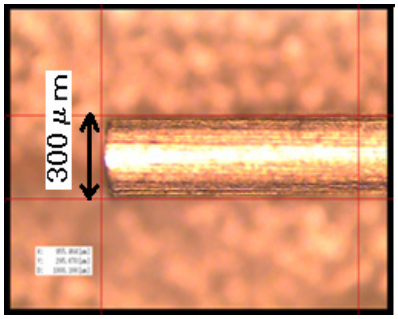

Fig. 18. φ300 needle (tungsten).

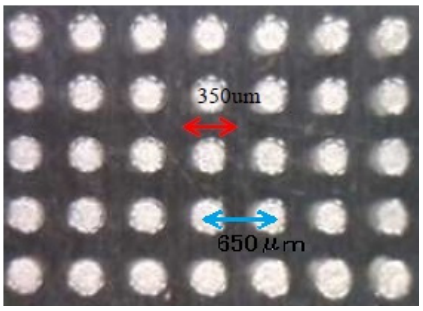

Fig. 19. Array of droplet (φ350).

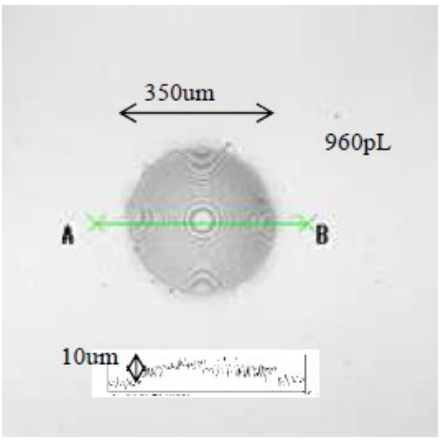

Fig. 20. Volume and thickness.

As an alternative experiment, a needle tip 10 μm in size was implemented, as shown in **Fig. 21**. The micro dispensing mechanism succeeded in providing a very small amount of highly viscous liquid (50,000 mPas, electrically conductive paste). This very small array of the micro droplet was achieved on the glass plate with a space of 50 μm, as shown in **Fig. 22**.

As shown in **Fig. 23**, the droplet diameter and the thickness were measured. It was found that the diameter is 12 μm and the thickness of the small liquid is 4 μm. Thus, the volume of the small liquid is calculated as 0.2 picoliters.

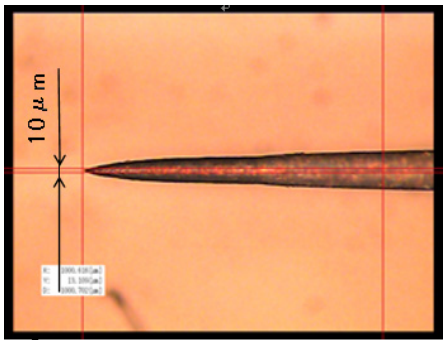

Fig. 21. φ10 needle (tungsten).

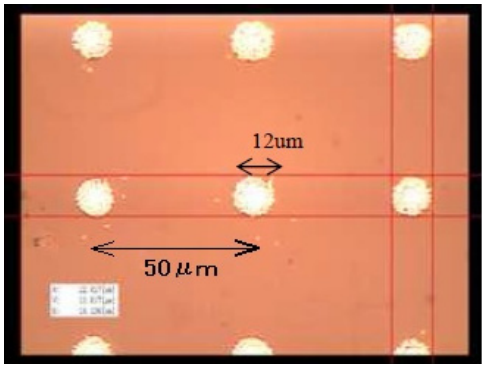

Fig. 22. Array of micro droplet (φ12).

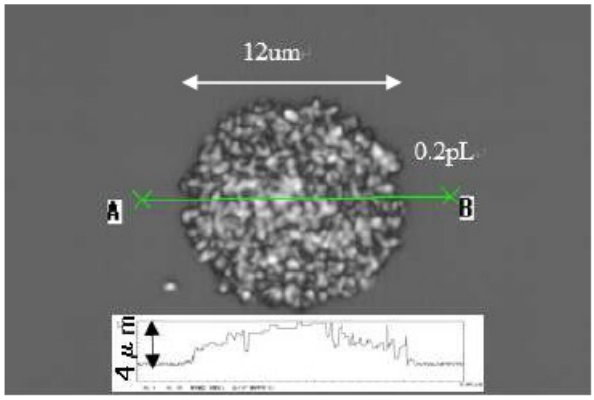

Fig. 23. Volume and thickness.

6. Conclusions

We developed a micro dispensing mechanism composed of a dispensing device and an XY stage that were inertially driven by piezoelectric elements.

We proposed a new waveform that combines the impulse and square waveforms to drive the moving slider. We compared the displacement, velocity, and acceleration of the new waveform with those of the sawtooth waveform. The acceleration of the sawtooth waveform caused an unstable slipping behaviour in the slider. The new waveform comprises a square waveform with an impulse signal added on the rising edge. It was considered that the inertial force was generated only once per cycle. The slider was successfully driven step-by-step with a microscopic displacement.

After combining the slider with the impact-driven XY stage, the array of the micro droplet was examined experimentally. When a needle tip 10 μm in diameter was implemented, the highly viscous liquid (50,000 mPas, electrically conductive paste) was successfully squeezed to the target. The droplet diameter and the thickness were measured, and it was found that the diameter was 12 μm and the thickness of the small liquid was 4 μm. Thus, the volume of this small liquid was estimated as 0.2 picoliters. It is well known that there are many parameters of dispensation, viscous, shape of needle tip, condition of target surface to decide the amount of the droplet. We are still considering the several conditions of dispensations and results.

References:

[1] T. Imai, "Printed Electronics," Fujikura Technical Review, Vol.2, pp. 63-66, 2012.

[2] K. Suzuki, K. Tsuji, A. Onodera, and T. Shibuya, "High-resolution Patterning Technologies using Ink-jet Printing and Laser Processing for Organic TFT Array," Society for imaging science and technology, NIP 29 and Digital Fabrication 2013, pp. 489-493, 2013.

[3] R. Yalla, K. P. Nayak, and K. Hakuta, "Fluorescence photon measurements from single quantum dots on an optical nanofiber," OPTICS EXPRESS, Vol.20, No.3, pp. 2932-2941, 2012.

[4] K. Suganuma, T. Kanzawa, D. Goto, J. Narui, and T. Otsuki, "Development of Printable Electronics for Circuit Formation," Fujitsu Ten Technical J., pp. 37-39, 2012.

[5] T. Seto, K. Takagi, K. Yoshida, J.-H. Park, and S. Yokota, "Development of High-Power Micropump Using Inertia Effect of Fluid for Small-Sized Fluid Actuators," J. of Robotics and Mechatronics, Vol.15, No.2, pp. 128-135, 2003.

[6] K. Yamamoto, H. Otaki, and Y. Ishikawa, "Moving mechanism using inertia," The Japan Society of Mechanical Engineers, Vol.57, pp. 1854-1859, 1991.

[7] H. Isobe, S. Kato, A. Kyusojin, and T. Moriguti, "Development of piezoelectric XYγ positioning device using impulsive force (2nd report) – Improvement of motion characteristic with friction control –," The Japan Society of Precision Engineering, Vol.64, No.3, pp. 408-412, 1998.

[8] Y. Nomura and H. Aoyama, "Development of Inertia Driven Micro Robot with Nano Tilting Stage for SEM Operation," Proc. of ASME/JSME Joint Conf. on Micromechanics for Information and Precision Equipment (MIPE 2006), 2006.

[9] M. Takizawa, Y. Irie, S. Hirata, and H. Aoyama, "Development of hemispherical manipulator and self-walking stage using piezoelectric actuator," 3rd Int. Conf. of Asian Society for Precision Engineering and Nanotechnology (ASPEN2009), Station Hotel Kokura, p. 1E6, 2009.

[10] H. Shiratori, M. Takizawa, Y. Irie, S. Hirata, and H. Aoyama, "Development of the Miniature Hemispherical Tilt Stage Driven by Stick-slip Motion using Piezoelectric Actuators," Mecatronics-REM2012, France, 2012.

[11] T. Higuchi and Y. Yamagata, "Micro robot arm utilizing rapid deformations of piezoelectric elements," J. of Robotics and Mechatronics, Vol.1, No.4, pp. 94-99, 1989.

[12] K. Uchino, "Piezoelectric actuators 2006 Expansion from IT/robotics to ecological/energy applications," J. Electroceram, Vol.20, pp. 301-311, 2008.

[13] Y. Tadano, R. Yoshida, and T, Morita, "Simulation modeling for resonance-type SIDM actuator," The Japan Society of Precision Engineering, pp. 183-184, 2013.

[14] NEC/TOKIN, "Multilayers piezoelectric actuators, Vol.07," Product catalog, p. 11.

[15] Y. Irie, J. Kubo, T. Fujioka, H. Aoyama, and T. Usuda, "Piezo-impact-driven X-Y stage and precise sample holder for accurate microlens alignment," J. of Rbotics and Mechatronics, Vol.21, No.5, pp. 635-641, 2009.

[16] S. Hirata, K. Hirose, Y. Irie, and H. Aoyama, "Evaluation of micro-gap control of the needle-type dispenser for precise micro-droplet dispensation," J. of Robotics and Mechatronics, Vol.25, No.5 pp. 848-854, 2013.

Name:
Yuuka Irie

Affiliation:
Ph.D. Student, The University of Electro-Communications

Address:
1-5-1 Chofugaoka, Chofu, Tokyo 182-8585, Japan

Brief Biographical History:
1994- NTT Advanced Technology Corporation
2006- Applied Micro Systems Inc.
2015- Department of Mechanical Engineering and Intelligent Systems, The University of Electro-Communications

Main Works:
• "Development of inertia driven nano X-Y stage for micro lens positioning," Asian Symposium for Precision Engineering and Nanotechnology, 2007.
• "Micro dispensing mechanism with vibrated taper needle and pipette," Asian Symposium for Precision Engineering and Nanotechnology, 2013.

Membership in Academic Societies:
• The Japan Society of Precision Engineering (JSPE)

Name:
Shinnosuke Hirata

Affiliation:
Assistant Professor, Department of Mechanical and Control Engineering, Tokyo Institute of Technology

Address:
S5-17, 2-12-1 Ookayama, Meguro-ku, Tokyo 152-8552, Japan

Brief Biographical History:
2009- Department of Mechanical Engineering and Intelligent Systems, The University of Electro-Communications
2012- Department of Mechanical and Control Engineering, Tokyo Institute of Technology

Main Works:
• S. Hirata, L. Haritaipan, K. Hoshiba, H. Hachiya, and N. Niimi, "Non-contact measurement of propagation speed in tissue-mimicking phantom using pass-through airborne ultrasound," Japanese J. of Applied Physics, Vol.53, No.7, p. 07KC17, 2014.

Membership in Academic Societies:
• The Institute of Electronics, Information and Communication Engineers (IEICE)
• The Acoustical Society of Japan (ASJ)
• The Institute of Electrical and Electronics Engineers (IEEE)
• The Japan Society of Ultrasonics in Medicine (JSUM)

Name:
Chisato Kanamori

Affiliation:
Associate Professor, Department of Mechanical Engineering and Intelligent Systems, Graduate School of Informatics and Engineering, The University of Electro-Communications

Address:
E4-303, 1-5-1 Chofugaoka, Chofu-shi, Tokyo 182-8585, Japan

Brief Biographical History:
1987/1989 Received B.E./M.E. from The University of Electro-Communications (UEC)
1991- Research Associate, UEC
2004- Received D.E. from UEC
2005- Associate Professor, UEC

Main Works:
• "Development of Intelligent Encoder," Proc. of The Twenty-third Annual Meeting of The American Society for Precision Engineering and the Twelfth ICPE (CD-ROM), #2639, Portland, USA, Oct. 21, 2008.

Membership in Academic Societies:
• The Japan Society of Mechanical Engineers (JSME)
• The Japan Society of Precision Engineering (JSPE)
• The Robotics Society of Japan (RSJ)

Name:
Hisayuki Aoyama

Affiliation:
Professor, Department of Mechanical Engineering and Intelligent Systems, The University of Electro-Communications

Address:
1-5-1 Chofugaoka, Chofu, Tokyo 182-8585, Japan

Brief Biographical History:
1983- Research Laboratory of Precision Machinery and Electronics, Tokyo Institute of Technology
1988- Department of Precision Engineering, Shizuoka University
1997- Department of Mechanical Engineering and Intelligent Systems, The University of Electro-Communications

Main Works:
• "Precise miniature robots and desktop flexible production," Proc. of Int. Workshop on Micro Factory, pp. 149-156, 1998.
• "Robust hybrid control for two-dimensional handheld micromanipulator," J. of Robotics and Mechatronics, Vol.26, No.3, pp. 331-340, 2014.